Two-dimensional liquid chromatography-mass spectrometry for lipidomics using off-line coupling of HILIC with 50 cm long reversed phase capillary columns

Matthew J. Sorensen[1], Kelsey E. Miller[2,3], James W. Jorgenson[3], Robert T. Kennedy[1,4]

1. Department of Chemistry, University of Michigan, Ann Arbor, MI 48109, USA
2. Current address: Center for Environmental Measurement and Modeling, U.S. Environmental Protection Agency, Research Triangle Park, NC 27709, USA
3. Department of Chemistry, University of North Carolina at Chapel Hill, Chapel Hill, NC 27599, USA
4. Department of Pharmacology, University of Michigan, Ann Arbor, MI 48109, USA

Corresponding Author: Robert Kennedy, rtkenn@umich.edu

Keywords:

Ultra-high pressure liquid chromatography

Two-dimensional chromatography

Lipidomics

Capillary liquid chromatography

Nanoscale liquid chromatography

Abstract

Comprehensive characterization of the lipidome remains a challenge requiring development of new analytical approaches to expand lipid coverage in complex samples. In this work, offline two-dimensional liquid chromatography-mass spectrometry was investigated for lipidomics from human plasma. Hydrophilic interaction liquid chromatography was implemented in the first dimension to fractionate lipid classes. Nine fractions were collected and subjected to a second dimension separation utilizing 50 cm capillary columns packed with 1.7 µm C18 particles operated on custom-built instrumentation at 35 kpsi. Online coupling with time-of-flight mass spectrometry allowed putative lipid identification from precursor-mass based library searching. The method had good orthogonality (fractional coverage of ~40%), achieved a peak capacity of approximately 1900 in 600 min, and detected over 1000 lipids from a 5 µL injection of a human plasma extract while consuming less than 3 mL of solvent. The results demonstrate the expected gains in peak capacity when employing long columns and two-dimensional separations, and illustrate practical approaches for improving lipidome coverage from complex biological samples.

1. Introduction

Lipidomics has emerged as an important technique for studying lipids from biological and environmental samples. Applications of lipidomics include studying disease states, physiological processes, pharmacological effects, and food science [1,2]. While targeted lipidomics can be valuable for studying and quantifying certain lipids for hypothesis-driven studies, untargeted approaches can give insight into how unknown or unexpected lipids are associated within the system of interest and can be used to generate new hypotheses [3,4]. Identifying and quantifying all lipids in a sample is challenging due to the large number, wide concentration range, numerous isomers, and broad physicochemical properties of lipids.

One analytical technique is not yet sufficient for analyzing an entire lipidome. Techniques implemented for untargeted lipidomics include spectroscopy and mass spectrometry, often coupled with separations [5]. Advantages of LC-MS based lipidomics include good resolving power, sensitivity, and amenability to a wide range of lipid classes [1,6–8]. Various approaches have been pursued to increase the lipidome coverage in LC-MS based lipidomics. Improving peak capacity of the separation is an important route to improving lipidome coverage, and multidimensional separations are a powerful approach for increasing peak capacity [9,10]. The theoretical peak capacity of a two-dimensional (2D) separation is the product of the first dimension (^{1}D) and second dimension (^{2}D) separation peak capacities, assuming the two separation mechanisms are orthogonal and the resolution of the first dimension is not compromised by the second dimension [10]. Multidimensional methods for lipids have demonstrated enhanced lipidome coverage relative to single dimensional analyses [11–16].

In 2D separations, transfer of effluent from the first dimension can occur online, where fractions are directed immediately to a rapid ^{2}D, or offline where fractions are collected and independently injected on the ^{2}D [17,18]. Online 2D-LC separations typically employ higher resolution ^{1}D separations and have the advantage of being fast; however, they come with a number of disadvantages [19]. Online 2D-LC typically involves more complicated instrumentation, worse detection limits due to dilution and (often) flow-splitting when coupled to MS, limited ^{2}D analysis time and peak capacity, and solvent incompatibility between the two dimensions [20,21]. In addition, for rapid methods the ^{2}D uses high flow rates and results in peak widths less than 1 s, which is too narrow to be accurately sampled by most mass spectrometers. These effects can lead to inaccurate peak width measurement, mass measurement, reduced sensitivity, and quantification. It also reduces the effectiveness of MS/MS methods such as data dependent acquisition where multiple MS scanning events need to occur within the elution band of a given compound. The incompatibility with MS constrains the possible applications of such on-line methods. Despite these

drawbacks, various online 2D-LC-MS methods have been developed for lipidomics with good separation peak capacity and lipidome coverage with analysis times typically 2 – 4 h [12,22–25].

Offline 2D-LC can overcome some of these challenges. Because the separations are independent, the ^{2}D analysis time is not limited by the ^{1}D peak width or sampling frequency. Thus, long gradients can be implemented in the ^{2}D, achieving high resolution separations with peak widths that are compatible with MS. Additionally, effluent from the first dimension can be dried down and resuspended in a more appropriate solvent for the ^{2}D. Finally, small resuspension volumes can preconcentrate fractions and provide enhanced signal intensity. Offline 2D-LC-MS approaches have typically provided broader lipidome coverage compared to online methods [11,16,26].

An intermediate approach is stop-flow 2D-LC. These methods do not require fast ^{2}D dimension separations, but are still mostly considered online [27]. This approach is still limited by solvent compatibility and more intricate instrument configuration relative to offline 2D-LC. Stop-flow 2D-LC is popular for proteomics with only a few reports for lipidomics [14,28].

Capillary LC with nanoESI-MS has also been implemented to increase lipidome coverage based on enhanced ionization efficiency and alleviation of ionization suppression associated with low flow rates [29–33]. Use of small inner diameter columns also reduces sample volume which can be beneficial for sample-limited analyses and reduces stationary and mobile phase consumption [34–36]. Capillary column formats also allow use of longer columns to be implemented without needing to couple multiple shorter columns. It is well known that long columns packed with small particles can provide much higher separation efficiencies; however, this approach requires high instrument operating pressure and is difficult to implement in a practical setting [37,38]. Recent reports of lipid separations have shown that use of long columns (e.g., 30 – 60 cm) packed with 1.7 µm C18 particles increased separation peak capacity for lipids, resolved more isomers, and detected more lipids in complex mixtures compared to lower resolution separations [39–42].

The combination of the strategies mentioned above (multidimensional separations, capillary LC-MS, and use of long columns) has recently been employed for various proteomic workflows in both top-down and bottom-up approaches [43–46]; however, there has been limited use of such technologies in lipidomics or metabolomics [15,47,48]. Here, we describe an offline 2D liquid chromatography-mass spectrometry method for untargeted lipidomics. Similar to previous work [11,49], we use a microbore bare silica HILIC column in the first dimension to separate lipid classes. Following evaporation and resuspension, each fraction was injected onto a 50 cm long x 100 µm bore column packed with 1.7 µm C18 particles operated at 35 kpsi interfaced to a quadrupole time-of-flight (QToF) mass spectrometer. Our

findings suggest large gains in peak capacity, compared to 1D approaches, that result in enhanced lipid coverage.

2. Materials and methods

2.1. Chemicals and standards

All solvents and chemicals were purchased from Sigma Aldrich (St. Louis, MO) unless otherwise stated. HPLC grade acetonitrile was purchased from Fisher Scientific (Waltham, MA). Potassium silicate (Kasil 2130) was purchased from PQ corporation (Valley Forge, IA). Palmitic acid was purchased from Sigma Aldrich. All other lipids were purchased from Avanti Polar Lipids Inc (Alabaster, AL).

2.2. Human plasma extraction

Pooled human plasma was provided by the Michigan Regional Comprehensive Metabolomics Resource Core. For lipid extraction, 50 µL of plasma, 200 µL of 0.15 M KCl in water, 400 µL of methanol, 200 µL of chloroform, and 1 µL of acetic acid were added to an Eppendorf tube and vortexed well [50]. An additional 200 µL of water and 200 µL of chloroform were added, vortexed briefly, and centrifuged at 12,100 × g for 5 min at room temperature. The organic layer was carefully collected and transferred to a glass HPLC vial, dried under nitrogen gas, and reconstituted in 100 µL of 90/10 (v/v) IPA/water for injection on the first dimension HILIC column.

2.3. First dimension HILIC-MS

Lipids were separated by HILIC in the first dimension using a 15 cm x 1 mm, 5 µm Spherisorb bare silica column (Waters; Milford, MA). A Waters NanoAcquity UPLC was used and coupled with a Micromass QToF Premier (Waters; Milford, MA). The method was similar to a previously reported method for lipid class separations [11,49]. Mobile phase A was 5 mM ammonium acetate and mobile phase B was acetonitrile. The flow rate was 50 µL/min. A gradient elution program was used as follows: initial, 95% B; 40 min, 77% B; 42 min, 95% B; 55 min, 95% B. The column oven was set to 30 °C. The injection volume was 5 µL. Electrospray ionization was used in positive ionization mode at 3.5 kV. The source temperature was 100 °C, desolvation temperature 150 °C, cone gas 50 L/h, and desolvation gas 450 L/h. The MS was operated in full scan mode from *m/z* 100 – 1000 with a 1 s scan rate and 0.1 s inter-scan.

For fraction collection, effluent from the ^{1}D separation was collected in glass HPLC vials. Fractions were typically collected in 1 – 2 min portions, which amounted to 50 – 100 µL of volume. Solvent was evaporated with a stream of nitrogen and re-dissolved in reversed phase mobile phase (different compositions and volumes depending on fraction type).

2.4. Capillary column packing

Polyimide-coated, fused silica capillaries with inner diameters (i.d.) of 100 µm and outer diameter (o.d.) of 360 µm were purchased from Polymicro Technologies, Inc. (Phoenix, AZ). Columns of 50 cm long x 100 µm i.d. were packed in-house with 1.7 µm C18 bridged ethyl hybrid particles (Waters; Milford, MA) as previously described [39,51]. Briefly, column outlet frits were prepared using the Kasil method [52]. An equal amount of potassium silicate and formamide were applied to a glass microfiber filter (Reeve Angel; Clifton, NJ) and the capillary tip was dabbed on the wetted paper to form the frit. A 200 mg/mL slurry was prepared in acetone and placed in an ultrahigh pressure packing apparatus. The column inlet was then secured and submerged in the slurry, with the rest of the column, other than the last ~2 cm, submerged in a sonication bath (Elma Schmidbauer GmbH; Singen, Germany). Packing was initiated by a DSHF-300 (Haskel; Burbank, CA) pneumatic amplifier pump at ~1000 psi, which displaced the loaded slurry with acetone. After ~2 cm of the column was packed, the pressure was increased to 30 kpsi. Once ~60 cm was packed, the column was slowly depressurized. The column was flushed at 50 kpsi for 1 h using a DSXHF-903 pump (Haskel; Burbank, CA), slowly depressurized, cut to 50 cm, and an inlet frit was applied using the Kasil method.

2.5. Second dimension RPLC-MS

Reversed phase LC separations were carried out on collected fractions using capillary LC-MS. Gradient elution was performed using a custom-built UHPLC system operated at a constant pressure of 35 kpsi using 50 cm x 100 µm, 1.7 µm C18 columns similar to previous reports [39,53]. Mobile phase A was 60/40 (v/v) water/acetonitrile with 10 mM ammonium formate and 0.1% (v/v) formic acid. Mobile phase B was 85/10/5 (v/v/v) isopropanol/acetonitrile/water with 10 mM ammonium formate and 0.1% (v/v) formic acid. Injection volumes were 1 or 2 µL. Injection solvent was 100% A for LPC and LPE fractions. For t_0 fraction, 100% B was used. For all other fractions, 50 or 100% B was used, with no major differences observed. For LPC and LPE fractions, the gradient was 50-70% B over 40 min. For PC and SM fractions, the gradient was 70-100% B over 70 min. For all other fractions, the gradient was 60-100% B over 60 min. The column temperature was 60 °C. Effluent from the column was transferred to either a Waters/Micromass QToF Premier or a Waters Xevo QToF using a stainless-steel union and a 30 µm i.d. spray tip (New Objective; Woburn, MA). For positive ionization mode, the spray voltage was 2 kV, cone voltage 30, the sheath gas was 0.5 bar, and the source temperature was 100 °C. For negative ionization mode, the spray voltage was 1.3 kV, cone voltage 22, and the sheath gas was 0.8 bar. The MS was operated in both full scan and MS/MS mode (MS^e and data-dependent acquisition). Scan rates were 0.3 s with 0.1 s inter-scan. External mass calibration was performed using sodium formate. Leucine enkephalin was used as the lock mass compound.

3. Results and discussion

3.1. First dimension HILIC separation

Previous work has shown that HILIC and RPLC were a useful and orthogonal combination for 2D-LC [11,12]. We used this combination with HILIC (15 cm long x 1 mm bore packed with 5 µm bare silica particles) as the ^{1}D for fractionation. A set of 14 lipid standards were used for method development (Figure 1A). Similar to previous reports, lipid separations utilizing bare silica particles for HILIC is dominated by the lipid head group so that a majority of lipid classes can be separated (Figure 1A) [49,54]. Certain isomers such as sn-1/sn-2 isomers of LPC and LPE are also resolved; however, because they can be separated with higher resolution by RP in the ^{2}D, they were collected in the same fraction to minimize total analysis time.

Similar resolution and peak shapes compared to the standards were achieved for endogenous lipids present in the plasma (**Figure 1B**). Importantly, good repeatability of retention times was achieved with subsequent injections of the plasma extract, ensuring successful collection of each fraction. Retention times were 1.86 ± 0.1, 13.75 ± 0.12, 25.35 ± 0.11, 29.04 ± 0.13, and 31.30 ± 0.19 min for fractions 1 (t_0), 4 (PE/PA), 7 (PC), 8 (SM), and 9 (LPC), respectively. Nine fractions were collected based on the elution profiles of different classes as summarized in **Supplemental Table 1**. The standard mixture did not contain representatives of all lipid classes that were found in plasma. These other classes include phosphatidylinositol phosphates, acyl-CoA's, and hexosylceramides, and were collected within the 9 fractions as summarized in Supplemental Table 1. The complexity of each fraction is illustrated in **Figure 2** where many ions are detected for a given peak during online ESI-MS analysis, demonstrating the potential need for ^{2}D separations of each fraction.

A disadvantage of employing bare silica columns is that most neutral and acidic lipids are not well separated. Fatty acids and neutral lipids such as glycerols and sterols/sterol esters elute in the dead time placing a greater burden on the separation of these components by reversed phase LC in the ^{2}D. Phosphatidic acids were retained but gave larger peak widths than the other lipid classes investigated (**Supplemental Figure 1**). Recent work has shown that hydride stationary phases can give improved separation of acidic lipids, however this was not investigated in this work [55]. Nonetheless, phosphatidic acids were still able to be collected with the phosphatidylethanolamine fraction and detected following ^{2}D RP-LC-MS analysis.

3.2. Evaluation of transfer from first to second dimension

One disadvantage of using an offline approach compared to online 2D-LC is the potential for analyte loss when transferring sample between the first and second dimensions. We evaluated the sample

recovery between the dimensions by comparing the signal of PC 18:1/18:1 standard injected directly onto the capillary column and injected on to the HILIC column, collected, evaporated, resuspended in ^{2}D buffer, and subsequently injected on to the capillary column. Peak height was 2705 ± 225 (n = 2 injections) and 3033 ± 435 (n = 3 injections) and peak area was 545 ± 53 and 573 ± 58 for the for the 2D workflow versus direct injection, respectively, suggesting no significant sample loss. Trace amounts of the most nonpolar lipids such as triacylglycerols and cholesteryl esters were seen in multiple fractions, possibly due to low solubility of TGs and CEs in the ^{1}D mobile phase, and the high concentration of these lipids in plasma (e.g., ~high µM to mM). Quantification could be problematic for these lipids as a result, and future work should investigate mitigation strategies.

3.3. Evaluation of ^{2}D injection amount

An advantage of offline 2D-LC is that the ^{2}D separations are independent of the ^{1}D allowing greater freedom regarding sample preparation and injection volume in the ^{2}D. We investigated different approaches for injecting larger amounts of each fraction on the ^{2}D column to increase detectability of more compounds. One approach was sample preconcentration. By reconstituting the fraction in a smaller volume after solvent evaporation from the first dimension, a more concentrated sample can be injected. **Figure 3A&B** illustrates the gain in signal intensity for fraction 2 (PGs and Ceramides) with no preconcentration compared to a 2X preconcentrated sample (sample redissolved in 20 µL vs. 10 µL, respectively) both with a 1 µL injection. Further preconcentration was attempted by redissolving in 5 µL; however, this approach was inconsistent likely due the difficulty in effectively dissolving the lipids. Additionally, this small of sample volume limits the number of possible replicates when using 1 – 2 µL injection volumes.

The second approach to maximizing the amount of lipids injected and detected was increasing the injection volume. Although the volume of the 50 cm x 100 µm capillary columns is ~3 µL, the high retention of lipids on C18 columns allowed relatively large injection volumes (1 – 2 µL) without detrimental loss in separation performance. Example base peak chromatograms for fraction 8 (sphingomyelins) shows a larger number of observed peaks and enhanced signal when using a 2 µL injection volume compared to 1 µL (**Figure 3C&D**). Limited sample available from fraction collection made it impractical to pursue larger sample volumes. These approaches for increasing the amount of sample injected on the ^{2}D were most beneficial for fractions with low lipid content or fractions that do not produce as good of MS response. In contrast, some fractions had sufficient content that injecting 2 µL results in frequent saturation of the MS detector. Supplemental Table 1 summarizes injection volumes and reconstitution volumes for each fraction.

3.4. Evaluation of ^{2}D gradient length and steepness

Previous work has shown that longer and shallower gradients improve the resolution and the number of lipids identified in untargeted single dimensional LC-MS lipidomics [39–41]. This observation is likely due to alleviation of ionization suppression caused by co-elution and increased resolution of isobaric species. Recent proteomics studies have shown that longer gradients are beneficial when injecting large amounts of sample (e.g., unfractionated and ng to µg amount of protein) but shorter gradients can be beneficial for sample-limited experiments where sensitivity losses from chromatographic dilution limit MS detection or when multidimensional separations decrease the sample complexity [56,57]. In pilot experiments, we evaluated the effect of gradient time and gradient slope on resolution and signal intensity of the lipid fractions. We compared 2-3 h gradient separations to ~1 h gradient times. For a few fractions a shorter gradient provided better signal intensity due to narrower peaks and higher peak heights from less chromatographic dilution (e.g., PG/Cer fraction, LPC fraction) compared to a ~2.5 h gradient (**Supplemental Figure 2**). In some cases, the broader peaks caused by such shallow gradients caused a loss in detection for lower abundance isomers (e.g., LPC 18:0 in the inset of **Supplemental Figure 2A&B**). For other fractions, however, a steeper gradient caused losses in resolution for certain critical pairs, and further method development was needed (**Figure 4A&C)**. Implementing a narrower Δ% B (e.g., 70 – 100% B) more amenable to the target compounds in each fraction allowed for shallower gradients to be used in roughly the same amount of time compared to wider gradient profiles (e.g., 50 – 100% B). This change provided good separation for isomeric and other critical pairs and was most evident in the fractions containing PCs and SMs (**Figure 4B&D**). Supplemental Table 1 summarizes the gradients used for each fraction based on these pilot experiment observations.

3.5. Orthogonality and 2D peak capacity measurements

Employing orthogonal separation mechanisms in a multidimensional separation is crucial for maximizing peak capacity [9,10]. In this work, we evaluated the orthogonality between the ^{1}D HILIC separation and the ^{2}D RP separations using the 'bin-containing' method [58,59]. In this approach, the separation space is divided into bins, and the fractional coverage is calculated by dividing the number of bins containing peaks by the total number of bins within the separation space. A bin was defined as 0.5 min wide, and a bin was considered at each point between the start and end of the gradient. A base peak chromatogram was generated for each fraction and the maximum intensity normalized to 100% (**Figure 5A**). A bin was considered "full" if the signal intensity was above 3% of the baseline. Results of this calculation are shown in **Figure 5B**. The coverage was determined to be 41%, which is considered highly orthogonal and thus the product rule of peak capacity measurement for a 2D separation is a good approximation [58]. A ~40% coverage space is similar to previous lipidomics reports using online HILIC and RP-LC [12].

The total peak capacity of the 2D-LC separation was 1880 with a total separation time of approximately 505 min for the 9 fractions plus 40 min for the ^{1}D separation (**Supplemental Table 1**). The t_0 fraction was analyzed twice (once in positive ion mode and once in negative ion mode), which made the total analysis time 605 min but did not increase the separation peak capacity. In terms of peak capacity repeatability, previous work using 50 cm columns showed good repeatability for unfractionated plasma extracts (~2-5% RSD) [39]. In this work several fractions were subjected to repeated analysis to ensure no large deviations in peak capacity. Peak capacity RSDs for fractions 1, 4, 8, and 9 were 1%, 8%, 6%, and 1% (n = 2), respectively.

3.6. Lipid identification

We putatively identified lipids from the human plasma extract using MS1 data and libraries from Lipid Blast [60] and the Metabolomics Workbench [61]. Approximately 1080 lipids were detected in human plasma using the 2D-LC-MS method. Peaks were identified based on fraction type, *m/z*, and retention time. Annotated ^{2}D chromatograms of fraction 7 (phosphatidylcholines) and fraction 9 (lysophosphatidylcholines) are shown in **Figure 6**. Other lipids were detected in these fractions but not labeled on the base peak chromatogram due to co-elution or signal below lower mass ions. These chromatograms illustrate the benefit of high resolution ^{2}D separations for detecting lipids from a complex mixture. Separation by chain length and double bond characteristics of lipid species is achieved within a given class as expected using reversed phase in the ^{2}D [41]. While comparisons with previous publications is difficult due to different instrumentation, matrices, and identification software used, the chromatograms here clearly show more peaks than previous 2D reports, indicating broader lipidome coverage.

The number of lipids detected is roughly double the number detected in our previous work using single dimensional RP-LC-MS at 35 kpsi with 3-4 h analysis time [39]. Similar improvements in lipid identification have been observed for multidimensional LC-MS lipidomics methods, likely due to decreased ionization suppression from higher peak capacity separations, cleaner mass spectra, and separation of isobaric and isomeric species [15,28]. As with peak capacity repeatability, lipid detection repeatability was examined for a few fractions to ensure no wide variations. The variation in lipids detected in fractions 1, 5, 7, and 9 were 18%, 33%, 5%, and 7% RSD (n = 2), similar to our previous report and suggesting no significant variability [39]. The improvement in detecting lipids and features by 2D comes at the expense of analysis time. Previous work with 1D separations showed an approximately linear increase in lipids and features detected with peak capacity and analysis time. The 2D data did not fit this trend, with fewer lipids and features detected per unit of peak capacity or analysis time (**Figure 7).** This work suggests a diminishing return in terms of lipid detection by increasing peak capacity. Without knowledge of the number of lipids present in the sample, it is difficult to know if this effect is due to actually resolving most of the lipids

available or limitations of the method. For example, dilution with longer methods may prevent detection of lower concentration lipids or the method may not be resolving more difficult to separate species due to insufficient selectivity.

Further improvements in lipidome coverage may be attainable using modified extraction protocols, employing smaller inner diameter columns with lower flow rates, combining with ion mobility separations and more sensitive mass spectrometers [13], or employing even higher resolution separations with smaller particles or longer columns [13,62]. Lipidome coverage could also be increased with the current instrumentation by selectively adjusting the ^{2}D mobile phase composition depending on the fraction type. For example, ammonium fluoride buffer provides higher signal intensity for PI species in negative ionization mode compared to ammonium formate or acetate buffers [63].

In this work 5 µL injection volumes, requiring 2.5 µL of undiluted plasma were used. These low volume injections are advantageous for small samples. The actual volume of plasma used in the extraction was 50 µL, and using smaller volumes of plasma (e.g., < 5 µL) may require different sample preparation techniques as discussed in other reports [31,46]. The use of a microbore column (1 mm i.d.) in the first dimension and a capillary column (100 µm i.d.) in the ^{2}D also provided low solvent consumption – approximately 2.5 mL in the total 2D-LC method.

3.7. Comparisons with previous 2D methods

Previous online 2D-LC lipidomics studies typically employed analysis times of 2 – 4 h, achieving peak capacities up to ~600 [16]. Using trapped ion mobility separations as ^{2}D, a peak capacity of 991 was achieved in 190 min, however lipid identifications were less than 2D-LC [12]. Offline 2D analysis times were typically > 5 h, with peak capacities estimated at ~500 – 1000 [11,26]. There has been little work implementing long capillary columns in the ^{2}D for lipidomics. High resolution 1D analyses of lipids have yielded peak capacities of 300 – 400 in 2 – 4 h using long (30 – 60 cm) columns [39–42]. Work shown here achieved peak capacities approaching 2000 and illustrates the advantages of long microcolumns for the ^{2}D for relatively high resolving power and peak capacity of lipids compared to previously published work.

Peak capacities for lipid separations are lower than what has been achieved with small molecules or peptides, likely due to the high viscosity of isopropanol-containing mobile phases which results in slower diffusion of lipids and limits particle size and column length. 1D peak capacities up to ~1800 can be achieved for peptides or small molecules using very long columns [53,64,65]. Recent online 2D-LC work for peptide separations has shown peak capacities of 1500 in 30 min and 10,000 in 240 min, although the extremely narrow peak widths are likely not compatible with most current MS methods [66,67].

4. Conclusions

Previous work has shown that 50 cm long columns packed with 1.7 μm particles and operated at 35 kpsi generate peak capacities up to 400 in 240 min and can detect up to ~500 lipids in plasma samples. We found that lipid prefractionation with HILIC into 9 fractions substantially increases the peak capacity to 1900 and number of lipids detected to 1100 for the capillary columns. Modification of 2D gradient parameters for individual fractions improved resolution and signal intensity compared to original conditions for unfractionated 1D analysis. The gain from prefractionation is likely more than would be possible by using even longer 1D columns and higher pressure due to the benefits of 2D separations including orthogonality, preconcentration, and multiplicity of peak capacity. Since the number of lipids detected did not increase proportionately with time, this work also illustrates the diminishing return of increasing analysis time for compounds identified. It is likely that more sensitive mass spectrometers could be used to further gain compound identifications in these mixtures. The long times are impractical for routine analysis, but this approach should be useful for characterizing samples in depth, especially if combined with MS/MS methods. Indeed, an important next step in this work will be to combine the high-resolution separation with MS/MS and standards to achieve more confident peak identification. Once confident compound identifications are obtained, it may be possible to use 1D methods to track the compounds for more routine quantitative work.

ACKNOWLEDGMENTS

This work was supported by NSF CHE-1904146 (R.T.K.). The authors thank Brady Anderson (University of Michigan) for helpful discussions. This work is not a product of the U.S. Government or U.S. EPA. The author, Kelsey Miller, did not do this work in any governmental capacity since her contribution was completed while at UNC Chapel Hill for graduate school. The views expressed are her own and do not necessarily represent those of the U.S. or U.S. EPA.

Figure Captions

Figure 1. First dimension HILIC separation of (A) lipid standards and (B) human plasma extract. Conditions: 15 cm x 1 mm, 5 µm bare silica column; 50 µL/min; 30 °C; 5 µL injection volume; 95-77% B gradient over 40 min; mobile phase A was 5 mM ammonium acetate; mobile phase B was acetonitrile. MS was operated in full scan positive ion mode. All effluent went to MS during these separations.

Figure 2. Example positive ion mode mass spectra of (A) fraction 7 (phosphatidylcholine) and (B) fraction 1 (glycerols, sterol esters, fatty acyls) following first dimension HILIC separation of human plasma with effluent directed online to the MS. Other LC-MS conditions are the same as in Figure 1.

Figure 3. Effect of resuspension volume and injection volume on signal intensity for different fractions. Comparison of 20 µL (A) and 10 µL (B) resuspension volumes on signal intensity for fraction 2 (phosphatidylglycerols and ceramides); gradient slope was 50-100% B. Comparison of 1 µL (C) and 2 µL (D) injection volumes on signal intensity for fraction 9 (sphingomyelins); gradient slope was 70-100% B. Other conditions: 50 cm x 100 µm, 1.7 µm C18 column; 35 kpsi operating pressure; 60 °C; mobile phase A was 60/40 water/acetonitrile with 10 mM ammonium formate and 0.1% formic acid; mobile phase B was 85/10/5 isopropanol/acetonitrile/water with 10 mM ammonium formate and 0.1% formic acid.

Figure 4. Effect of gradient steepness on chromatographic resolution for (A and B) fraction 7 (phosphatidylcholines) and (C and D) fraction 8 (sphingomyelins). A 50-100% B gradient (A) is compared with a 70-100% B gradient (B). Example EICs for *m/z* 784.6 and 786.6 are shown to illustrate the improvement in resolution of different isomers with a shallower gradient. A 60-100% B gradient over 50 min (C) is compared with a 70-100% B gradient over 70 min (D). EICs for *m/z* 813 and 811 are shown. Other conditions are the same as in Figure 3.

Figure 5. (A) Two-dimensional waterfall plot with each fraction displayed as base peak intensity chromatograms. Individual LC-MS parameters are in the text and from Figure 3. (B) "bin"-based fractional coverage plot used for orthogonality measurement.

Figure 6. Base peak chromatograms of (A) fraction 7 (phosphatidylcholine) and (B) fraction 9 (lysophosphatidylcholine) with peaks annotated with the identified lipid based on *m/z* and retention time. For fraction 7, a 70-100% B gradient was used; for fraction 9, a 50-70% B gradient was used. Other conditions are the same as in Figure 3.

Figure 7. Number of lipids detected and MS1 features detected from previous 1D LC-MS work (black circles) and the present 2D work (gray diamond). Lipids identified using library database matching of precursor ion data is plotted as a function of peak capacity (A) and analysis time (B). MS1 features are plotted versus peak capacity (C) and analysis time (D). One-dimensional work is reproduced in part from previous work.

391 **Figures**

392 **Figure 1.**

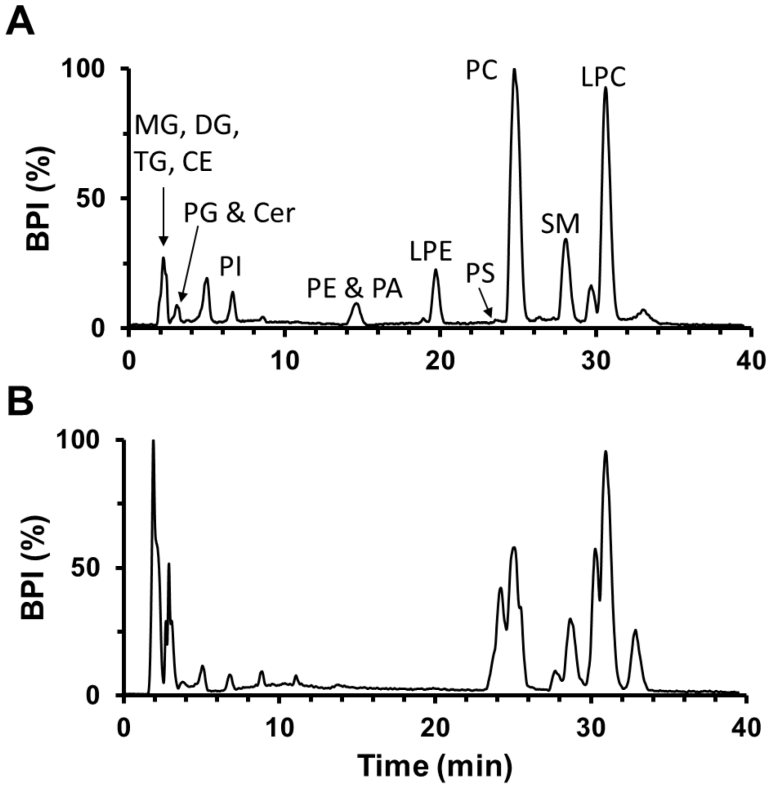

393

394

395 **Figure 2.**

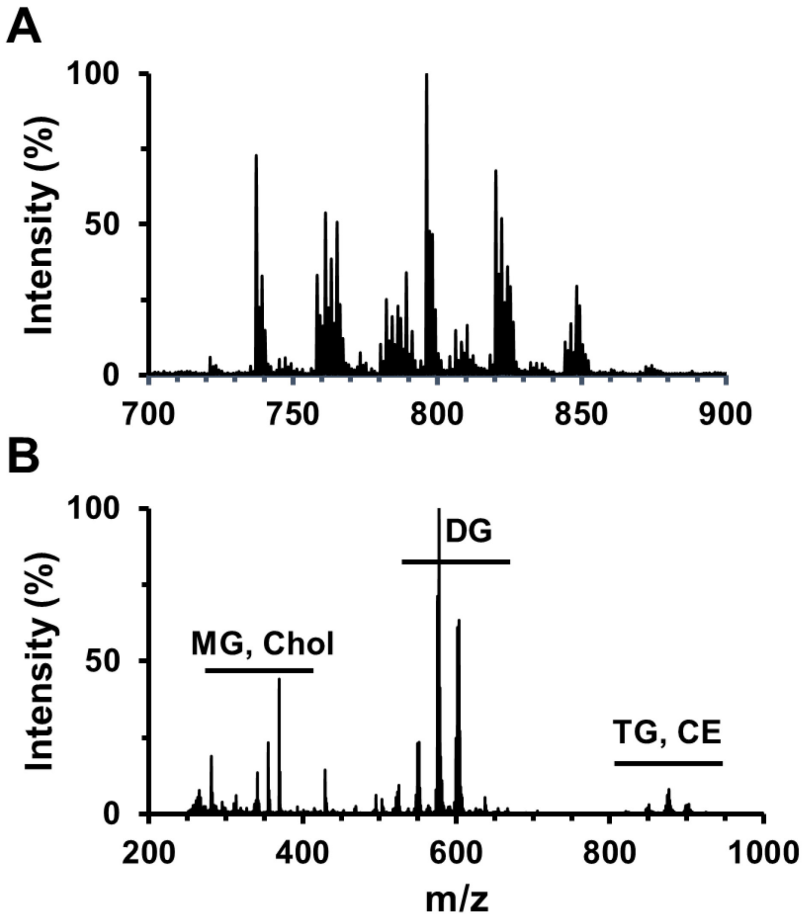

396

397

398

399

400 **Figure 3.**

401

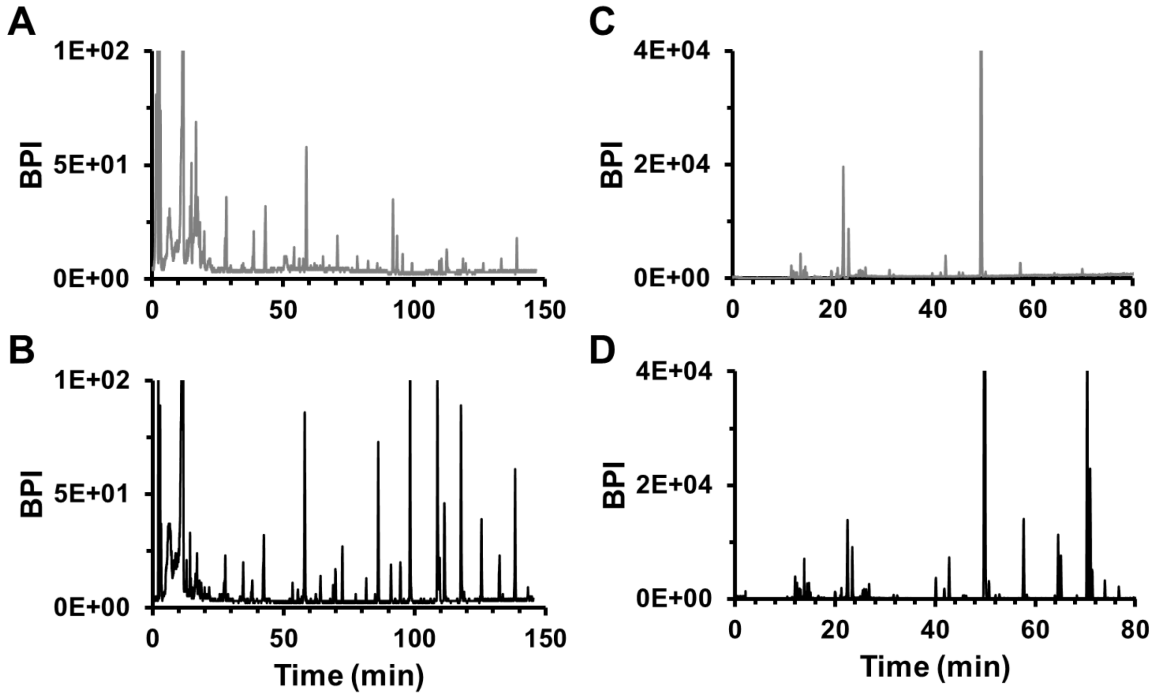

402

403

404

405

406 **Figure 4.**

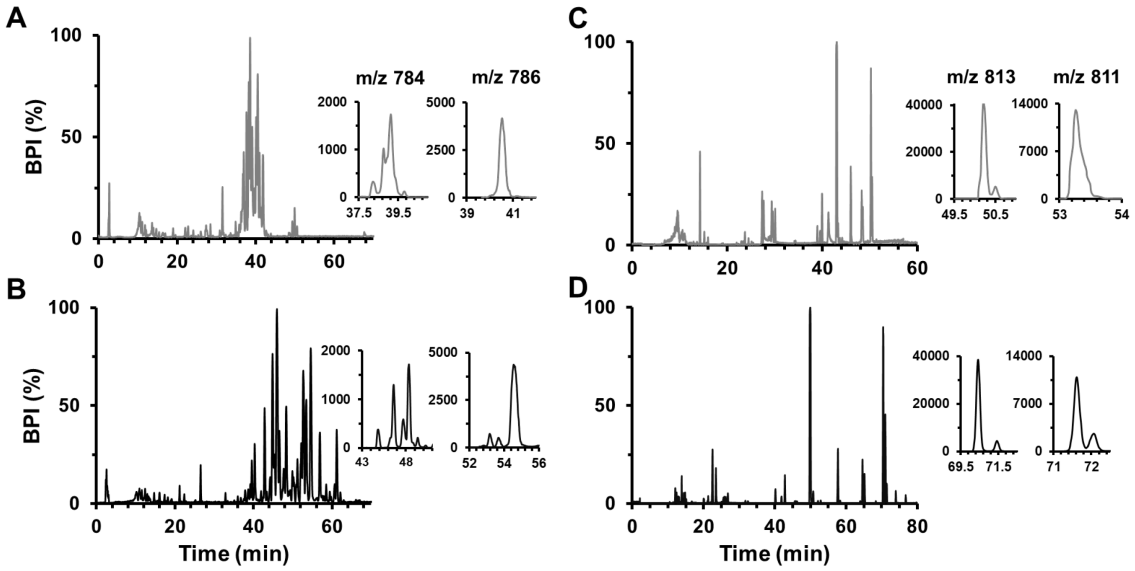

407

408

409

410 **Figure 5.**

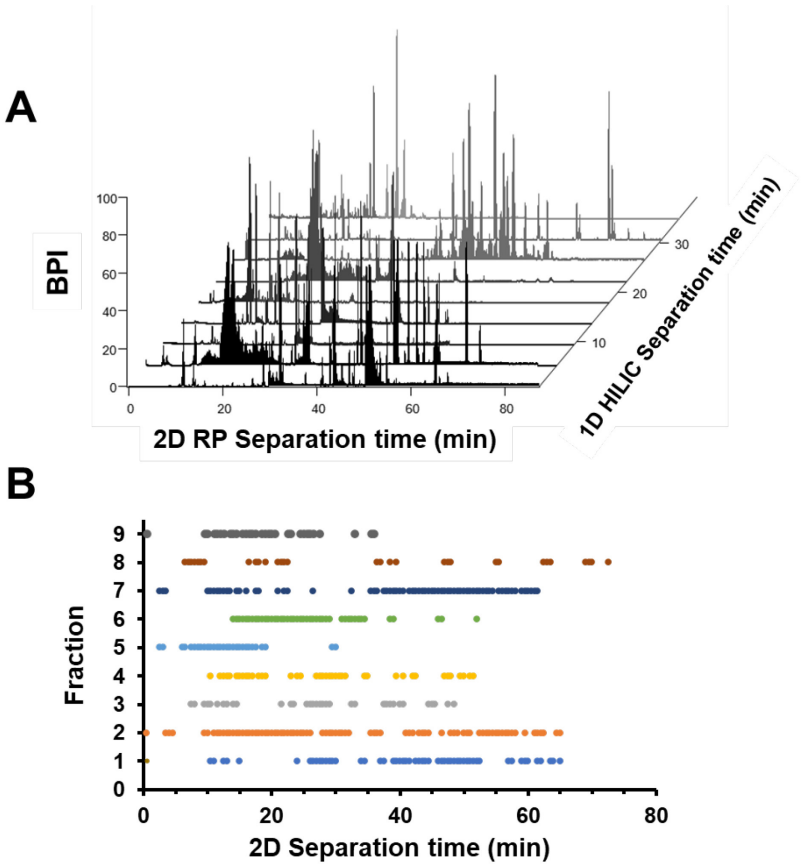

411

412

413 **Figure 6.**

414

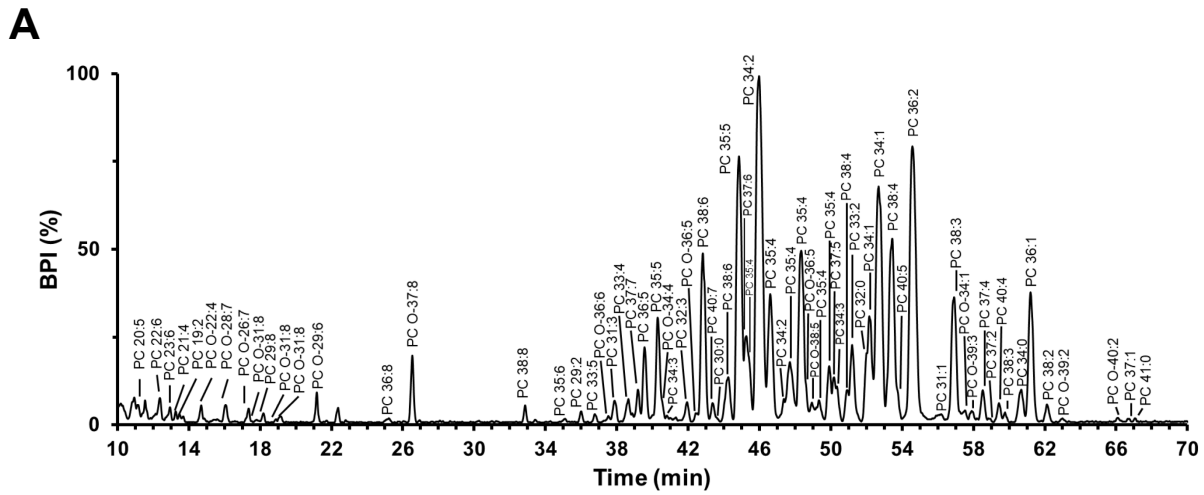

415

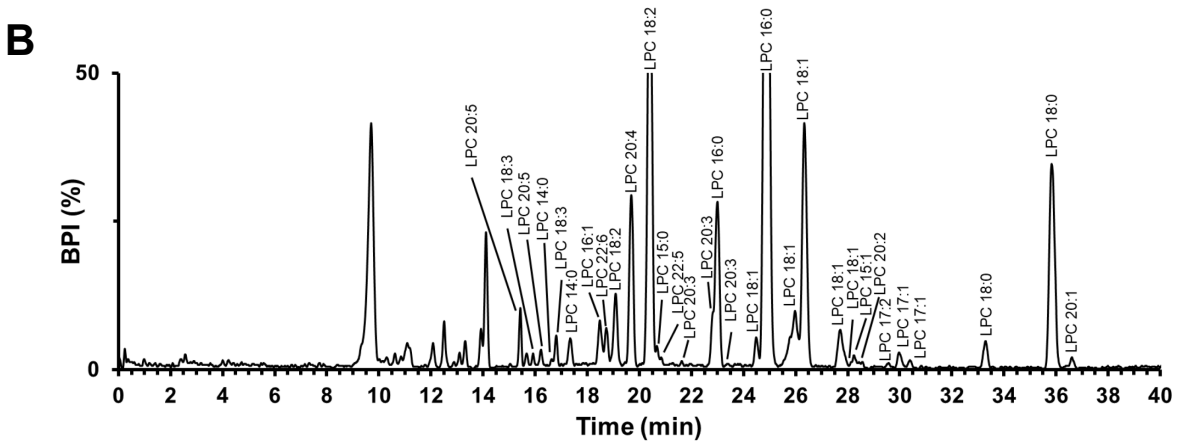

416

417

418 **Figure 7**

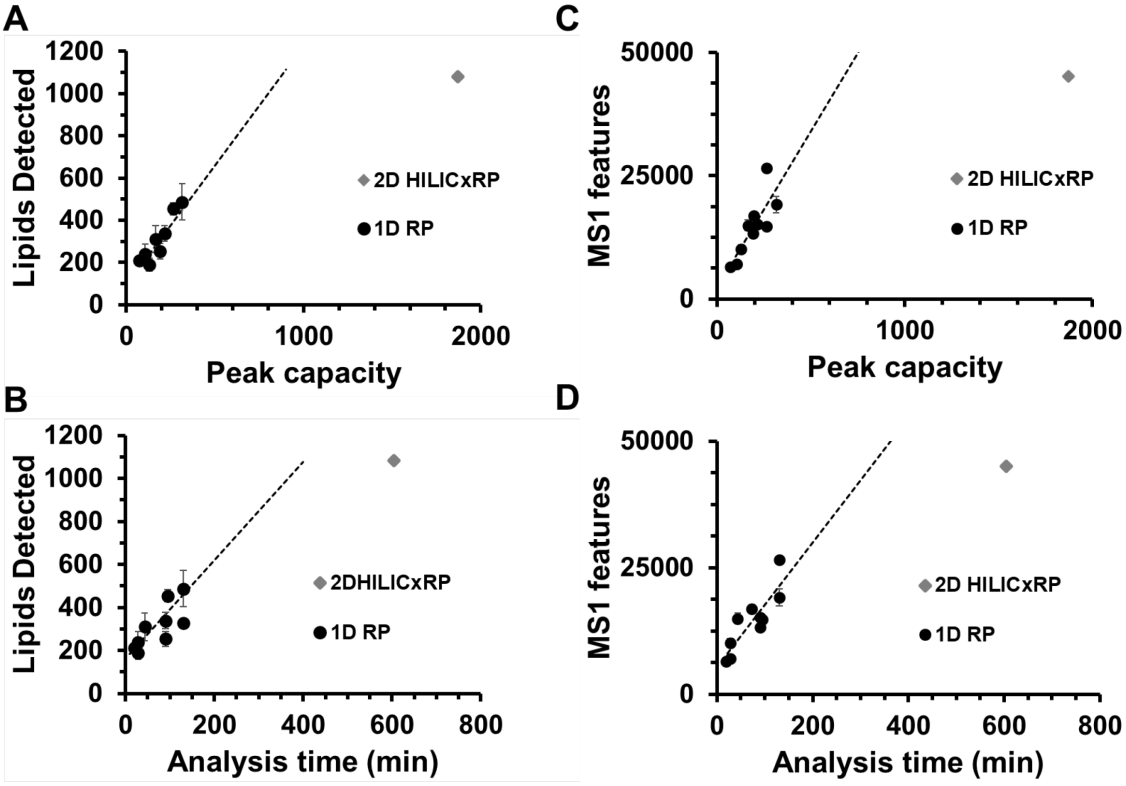

419

Supplemental Material

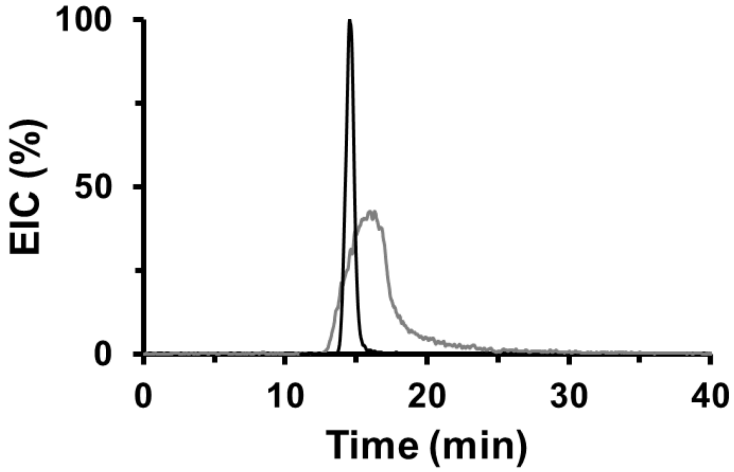

Supplemental Figure S1. Poor peak shape of phosphatidic acid (gray) on the [1]D bare silica column. Phosphatidylethanolamine (black), which co-eluted and was collected with phosphatidic acid, demonstrated better peak shape representative of most lipids on this column.

Supplemental Table 1. Conditions used for fraction collection of different lipid classes and analysis of each fraction in second dimension.

Fraction	Lipid class(es)	Collection time (min)	Reconstitution volume (µL)	Injection volume (µL)	^{2}D gradient slope (%ΔB)	^{2}D gradient time (min)	Peak capacity
1	TG, DG, MG, FA, Chol, CE, acylCoA, PIP	1.3-3	10	2	60-100	60	275
2	PG, Cer	3-5	10	2	60-100	70	285
3	PI, HexCer, LPG	5-8	10	2	60-100	60	265
4	PE, PA	13-16	10	2	60-100	50	205
5	LPE	18.5-21	10	2	50-70	40	145
6	PS	21.5-23	10	2	60-100	50	155
7	PC	23-26	20	1	70-100	65	145
8	SM	27-29.5	20	2	70-100	70	241
9	LPC	29.5-32.5	20	1	50-70	40	163

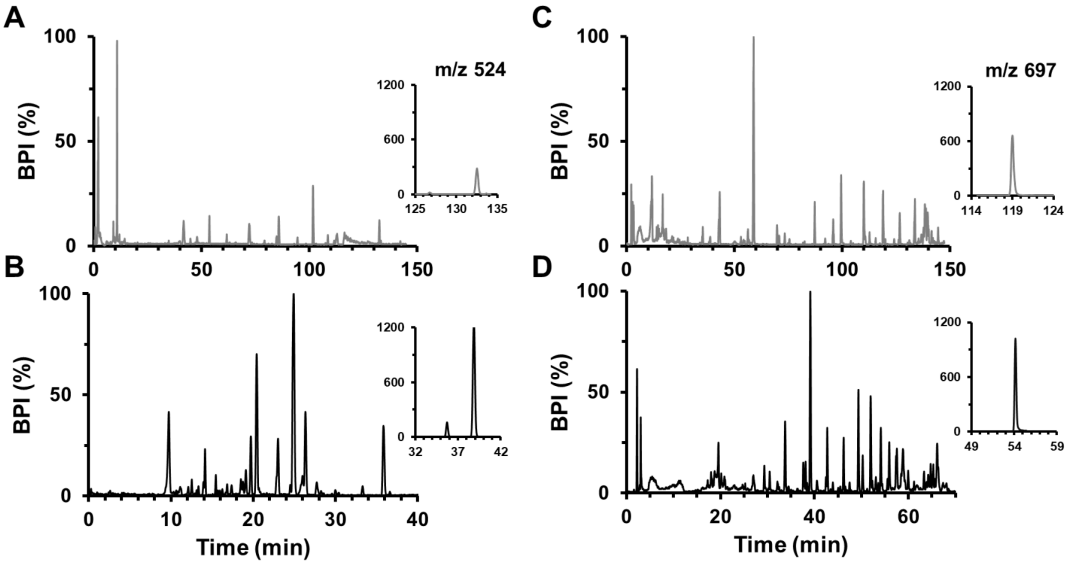

Supplemental Figure 2. Effect of gradient length for (A & B) fractions 9 (lysophosphatidylcholine) and (C & D) fraction 2 (phosphatidylglycerols and ceramides). A longer ~2.5 h gradient (A & C) is compared with ~ 1 h gradient (B & D). Example extracted ion chromatograms show the decrease in signal height at longer gradient times.

References

[1] H.F. Avela, H. Sirén, Advances in lipidomics, Clinica Chimica Acta. 510 (2020) 123–141. https://doi.org/10.1016/j.cca.2020.06.049.

[2] H.-C. Lee, T. Yokomizo, Applications of mass spectrometry-based targeted and non-targeted lipidomics, Biochemical and Biophysical Research Communications. 504 (2018) 576–581. https://doi.org/10.1016/j.bbrc.2018.03.081.

[3] A. Kruve, Strategies for Drawing Quantitative Conclusions from Nontargeted Liquid Chromatography–High-Resolution Mass Spectrometry Analysis, Anal. Chem. 92 (2020) 4691–4699. https://doi.org/10.1021/acs.analchem.9b03481.

[4] T. Cajka, O. Fiehn, Toward Merging Untargeted and Targeted Methods in Mass Spectrometry-Based Metabolomics and Lipidomics, Anal. Chem. 88 (2016) 524–545. https://doi.org/10.1021/acs.analchem.5b04491.

[5] K. Jurowski, K. Kochan, J. Walczak, M. Barańska, W. Piekoszewski, B. Buszewski, Analytical Techniques in Lipidomics: State of the Art, Critical Reviews in Analytical Chemistry. 47 (2017) 418–437. https://doi.org/10.1080/10408347.2017.1310613.

[6] S. Tumanov, J.J. Kamphorst, Recent advances in expanding the coverage of the lipidome, Current Opinion in Biotechnology. 43 (2017) 127–133. https://doi.org/10.1016/j.copbio.2016.11.008.

[7] Y.H. Rustam, G.E. Reid, Analytical Challenges and Recent Advances in Mass Spectrometry Based Lipidomics, Analytical Chemistry. 90 (2018) 374–397. https://doi.org/10.1021/acs.analchem.7b04836.

[8] E. Rampler, Y.E. Abiead, H. Schoeny, M. Rusz, F. Hildebrand, V. Fitz, G. Koellensperger, Recurrent Topics in Mass Spectrometry-Based Metabolomics and Lipidomics—Standardization, Coverage, and Throughput, Anal. Chem. 93 (2021) 519–545. https://doi.org/10.1021/acs.analchem.0c04698.

[9] J.C. Giddings, Concepts and comparisons in multidimensional separation, J. High Resol. Chromatogr. 10 (1987) 319–323. https://doi.org/10.1002/jhrc.1240100517.

[10] J.C. Giddings, Two-dimensional separations: concept and promise, Anal. Chem. 56 (1984) 1258A-1270A. https://doi.org/10.1021/ac00276a003.

[11] M. Lísa, E. Cífková, M. Holčapek, Lipidomic profiling of biological tissues using off-line two-dimensional high-performance liquid chromatography–mass spectrometry, Journal of Chromatography A. 1218 (2011) 5146–5156. https://doi.org/10.1016/j.chroma.2011.05.081.

[12] A. Baglai, A.F.G. Gargano, J. Jordens, Y. Mengerink, M. Honing, S. van der Wal, P.J. Schoenmakers, Comprehensive lipidomic analysis of human plasma using multidimensional liquid- and gas-phase separations: Two-dimensional liquid chromatography–mass spectrometry vs . liquid chromatography–trapped-ion-mobility–mass spectrometry, Journal of Chromatography A. 1530 (2017) 90–103. https://doi.org/10.1016/j.chroma.2017.11.014.

[13] I. Blaženović, T. Shen, S.S. Mehta, T. Kind, J. Ji, M. Piparo, F. Cacciola, L. Mondello, O. Fiehn, Increasing Compound Identification Rates in Untargeted Lipidomics Research with Liquid Chromatography Drift Time–Ion Mobility Mass Spectrometry, Analytical Chemistry. 90 (2018) 10758–10764. https://doi.org/10.1021/acs.analchem.8b01527.

[14] P. Dugo, N. Fawzy, F. Cichello, F. Cacciola, P. Donato, L. Mondello, Stop-flow comprehensive two-dimensional liquid chromatography combined with mass spectrometric detection for phospholipid analysis, Journal of Chromatography A. 1278 (2013) 46–53. https://doi.org/10.1016/j.chroma.2012.12.042.

[15] D.Y. Bang, M.H. Moon, On-line two-dimensional capillary strong anion exchange/reversed phase liquid chromatography–tandem mass spectrometry for comprehensive lipid analysis, Journal of Chromatography A. 1310 (2013) 82–90. https://doi.org/10.1016/j.chroma.2013.08.069.

[16] W. Lv, X. Shi, S. Wang, G. Xu, Multidimensional liquid chromatography-mass spectrometry for metabolomic and lipidomic analyses, TrAC Trends in Analytical Chemistry. 120 (2019) 115302. https://doi.org/10.1016/j.trac.2018.11.001.
[17] K.M. Kalili, A. de Villiers, Systematic optimisation and evaluation of on-line, off-line and stop-flow comprehensive hydrophilic interaction chromatography×reversed phase liquid chromatographic analysis of procyanidins, Part I: Theoretical considerations, Journal of Chromatography A. 1289 (2013) 58–68. https://doi.org/10.1016/j.chroma.2013.03.008.
[18] G. Guiochon, N. Marchetti, K. Mriziq, R.A. Shalliker, Implementations of two-dimensional liquid chromatography, Journal of Chromatography A. 1189 (2008) 109–168. https://doi.org/10.1016/j.chroma.2008.01.086.
[19] D.R. Stoll, P.W. Carr, Two-Dimensional Liquid Chromatography: A State of the Art Tutorial, Anal. Chem. 89 (2017) 519–531. https://doi.org/10.1021/acs.analchem.6b03506.
[20] B.W.J. Pirok, D.R. Stoll, P.J. Schoenmakers, Recent Developments in Two-Dimensional Liquid Chromatography: Fundamental Improvements for Practical Applications, Anal. Chem. 91 (2019) 240–263. https://doi.org/10.1021/acs.analchem.8b04841.
[21] P.J. Schoenmakers, B.W.J. Pirok, Practical Approaches to Overcome the Challenges of Comprehensive Two-Dimensional Liquid Chromatography, LCGC Eurpoe. 31 (2018) 242–249.
[22] M. Holčapek, M. Ovčačíková, M. Lísa, E. Cífková, T. Hájek, Continuous comprehensive two-dimensional liquid chromatography–electrospray ionization mass spectrometry of complex lipidomic samples, Analytical and Bioanalytical Chemistry. 407 (2015) 5033–5043. https://doi.org/10.1007/s00216-015-8528-2.
[23] M. Navarro-Reig, J. Jaumot, R. Tauler, An untargeted lipidomic strategy combining comprehensive two-dimensional liquid chromatography and chemometric analysis, Journal of Chromatography A. 1568 (2018) 80–90. https://doi.org/10.1016/j.chroma.2018.07.017.
[24] M. Li, X. Tong, P. Lv, B. Feng, L. Yang, Z. Wu, X. Cui, Y. Bai, Y. Huang, H. Liu, A not-stop-flow online normal-/reversed-phase two-dimensional liquid chromatography–quadrupole time-of-flight mass spectrometry method for comprehensive lipid profiling of human plasma from atherosclerosis patients, Journal of Chromatography A. 1372 (2014) 110–119. https://doi.org/10.1016/j.chroma.2014.10.094.
[25] H. Nie, R. Liu, Y. Yang, Y. Bai, Y. Guan, D. Qian, T. Wang, H. Liu, Lipid profiling of rat peritoneal surface layers by online normal- and reversed-phase 2D LC QToF-MS[S], Journal of Lipid Research. 51 (2010) 2833–2844. https://doi.org/10.1194/jlr.D007567.
[26] M. Narváez-Rivas, N. Vu, G.-Y. Chen, Q. Zhang, Off-line mixed-mode liquid chromatography coupled with reversed phase high performance liquid chromatography-high resolution mass spectrometry to improve coverage in lipidomics analysis, Analytica Chimica Acta. 954 (2017) 140–150. https://doi.org/10.1016/j.aca.2016.12.003.
[27] D.A. Wolters, M.P. Washburn, J.R. Yates, An Automated Multidimensional Protein Identification Technology for Shotgun Proteomics, Anal. Chem. 73 (2001) 5683–5690. https://doi.org/10.1021/ac010617e.
[28] S. Wang, J. Li, X. Shi, L. Qiao, X. Lu, G. Xu, A novel stop-flow two-dimensional liquid chromatography–mass spectrometry method for lipid analysis, Journal of Chromatography A. 1321 (2013) 65–72. https://doi.org/10.1016/j.chroma.2013.10.069.
[29] N. Danne-Rasche, C. Coman, R. Ahrends, Nano-LC/NSI MS Refines Lipidomics by Enhancing Lipid Coverage, Measurement Sensitivity, and Linear Dynamic Range, Analytical Chemistry. 90 (2018) 8093–8101. https://doi.org/10.1021/acs.analchem.8b01275.
[30] N. Danne-Rasche, S. Rubenzucker, R. Ahrends, Uncovering the complexity of the yeast lipidome by means of nLC/NSI-MS/MS, Analytica Chimica Acta. 1140 (2020) 199–209. https://doi.org/10.1016/j.aca.2020.10.012.

[31] A. Zardini Buzatto, B.K. Kwon, L. Li, Development of a NanoLC-MS workflow for high-sensitivity global lipidomic analysis, Analytica Chimica Acta. 1139 (2020) 88–99. https://doi.org/10.1016/j.aca.2020.09.001.
[32] S.K. Byeon, J.Y. Lee, M.H. Moon, Optimized extraction of phospholipids and lysophospholipids for nanoflow liquid chromatography-electrospray ionization-tandem mass spectrometry, Analyst. 137 (2012) 451–458. https://doi.org/10.1039/c1an15920h.
[33] G.B. Lee, J.C. Lee, M.H. Moon, Plasma lipid profile comparison of five different cancers by nanoflow ultrahigh performance liquid chromatography-tandem mass spectrometry, Analytica Chimica Acta. 1063 (2019) 117–126. https://doi.org/10.1016/j.aca.2019.02.021.
[34] K.L. Sanders, J.L. Edwards, Nano-liquid chromatography-mass spectrometry and recent applications in omics investigations, Anal. Methods. 12 (2020) 4404–4417. https://doi.org/10.1039/D0AY01194K.
[35] K.D. Duncan, J. Fyrestam, I. Lanekoff, Advances in mass spectrometry based single-cell metabolomics, Analyst. 144 (2019) 782–793. https://doi.org/10.1039/C8AN01581C.
[36] J. Stadlmann, O. Hudecz, G. Krššáková, C. Ctortecka, G. Van Raemdonck, J. Op De Beeck, G. Desmet, J.M. Penninger, P. Jacobs, K. Mechtler, Improved Sensitivity in Low-Input Proteomics Using Micropillar Array-Based Chromatography, Anal. Chem. 91 (2019) 14203–14207. https://doi.org/10.1021/acs.analchem.9b02899.
[37] M.J. Sorensen, B.G. Anderson, R.T. Kennedy, Liquid chromatography above 20,000 PSI, TrAC Trends in Analytical Chemistry. 124 (2020) 115810. https://doi.org/10.1016/j.trac.2020.115810.
[38] K. Broeckhoven, G. Desmet, Advances and Challenges in Extremely High-Pressure Liquid Chromatography in Current and Future Analytical Scale Column Formats, Anal. Chem. 92 (2020) 554–560. https://doi.org/10.1021/acs.analchem.9b04278.
[39] M.J. Sorensen, K.E. Miller, J.W. Jorgenson, R.T. Kennedy, Ultrahigh-Performance capillary liquid chromatography-mass spectrometry at 35 kpsi for separation of lipids, Journal of Chromatography A. 1611 (2020) 460575. https://doi.org/10.1016/j.chroma.2019.460575.
[40] K.E. Miller, J.W. Jorgenson, Comparison of microcapillary column length and inner diameter investigated with gradient analysis of lipids by ultrahigh-pressure liquid chromatography-mass spectrometry, J. Sep. Sci. (2020) jssc.202000545. https://doi.org/10.1002/jssc.202000545.
[41] M. Ovčačíková, M. Lísa, E. Cífková, M. Holčapek, Retention behavior of lipids in reversed-phase ultrahigh-performance liquid chromatography–electrospray ionization mass spectrometry, Journal of Chromatography A. 1450 (2016) 76–85. https://doi.org/10.1016/j.chroma.2016.04.082.
[42] K. Sandra, J. Vandenbussche, R. t'Kindt, B. Claerebout, J. Op de Beeck, W. De Malsche, G. Desmet, P. Sandra, Evaluation of Micro-Pillar Array Columns (µPAC) Combined with High Resolution Mass Spectrometry for Lipidomics, LCGC. 30 (2017) 6–13.
[43] A. Motoyama, J.D. Venable, C.I. Ruse, J.R. Yates, Automated Ultra-High-Pressure Multidimensional Protein Identification Technology (UHP-MudPIT) for Improved Peptide Identification of Proteomic Samples, Analytical Chemistry. 78 (2006) 5109–5118. https://doi.org/10.1021/ac060354u.
[44] Z. Wang, D. Yu, K.A. Cupp-Sutton, X. Liu, K. Smith, S. Wu, Development of an Online 2D Ultrahigh-Pressure Nano-LC System for High-pH and Low-pH Reversed Phase Separation in Top-Down Proteomics, Anal. Chem. 92 (2020) 12774–12777. https://doi.org/10.1021/acs.analchem.0c03395.
[45] D. Yu, Z. Wang, K.A. Cupp-Sutton, X. Liu, S. Wu, Deep Intact Proteoform Characterization in Human Cell Lysate Using High-pH and Low-pH Reversed-Phase Liquid Chromatography, J. Am. Soc. Mass Spectrom. 30 (2019) 2502–2513. https://doi.org/10.1007/s13361-019-02315-2.
[46] M. Dou, C.-F. Tsai, P.D. Piehowski, Y. Wang, T.L. Fillmore, R. Zhao, R.J. Moore, P. Zhang, W.-J. Qian, R.D. Smith, T. Liu, R.T. Kelly, T. Shi, Y. Zhu, Automated Nanoflow Two-Dimensional Reversed-Phase Liquid Chromatography System Enables In-Depth Proteome and Phosphoproteome Profiling of

583 Nanoscale Samples, Anal. Chem. 91 (2019) 9707–9715.
584 https://doi.org/10.1021/acs.analchem.9b01248.
585 [47] J.D. Vos, D. Stoll, S. Buckenmaier, S. Eeltink, J.P. Grinias, Advances in ultra-high-pressure and multi-
586 dimensional liquid chromatography instrumentation and workflows, Analytical Science Advances.
587 2 (2021) 171–192. https://doi.org/10.1002/ansa.202100007.
588 [48] M. Lísa, H. Řehulková, E. Hančová, P. Řehulka, Lipidomic Analysis Using Hydrophilic Interaction
589 Liquid Chromatography Microgradient Fractionation of Total Lipid Extracts, Journal of
590 Chromatography A. (2021) 462380. https://doi.org/10.1016/j.chroma.2021.462380.
591 [49] E. Cífková, M. Holčapek, M. Lísa, M. Ovčačíková, A. Lyčka, F. Lynen, P. Sandra, Nontargeted
592 Quantitation of Lipid Classes Using Hydrophilic Interaction Liquid Chromatography–Electrospray
593 Ionization Mass Spectrometry with Single Internal Standard and Response Factor Approach,
594 Analytical Chemistry. 84 (2012) 10064–10070. https://doi.org/10.1021/ac3024476.
595 [50] E.G. Bligh, W.J. Dyer, A RAPID METHOD OF TOTAL LIPID EXTRACTION AND PURIFICATION, Canadian
596 Journal of Biochemistry and Physiology. 37 (1959) 911–917. https://doi.org/10.1139/o59-099.
597 [51] J.M. Godinho, A.E. Reising, U. Tallarek, J.W. Jorgenson, Implementation of high slurry
598 concentration and sonication to pack high-efficiency, meter-long capillary ultrahigh pressure liquid
599 chromatography columns, Journal of Chromatography A. 1462 (2016) 165–169.
600 https://doi.org/10.1016/j.chroma.2016.08.002.
601 [52] A. Maiolica, D. Borsotti, J. Rappsilber, Self-made frits for nanoscale columns in proteomics,
602 PROTEOMICS. 5 (2005) 3847–3850. https://doi.org/10.1002/pmic.200402010.
603 [53] K.M. Grinias, J.M. Godinho, E.G. Franklin, J.T. Stobaugh, J.W. Jorgenson, Development of a 45kpsi
604 ultrahigh pressure liquid chromatography instrument for gradient separations of peptides using
605 long microcapillary columns and sub-2µm particles, Journal of Chromatography A. 1469 (2016) 60–
606 67. https://doi.org/10.1016/j.chroma.2016.09.053.
607 [54] M. Schwalbe-Herrmann, J. Willmann, D. Leibfritz, Separation of phospholipid classes by hydrophilic
608 interaction chromatography detected by electrospray ionization mass spectrometry, Journal of
609 Chromatography A. 1217 (2010) 5179–5183. https://doi.org/10.1016/j.chroma.2010.05.014.
610 [55] E. Cífková, R. Hájek, M. Lísa, M. Holčapek, Hydrophilic interaction liquid chromatography-mass
611 spectrometry of (lyso)phosphatidic acids, (lyso)phosphatidylserines and other lipid classes, Journal
612 of Chromatography A. 1439 (2016) 65–73. https://doi.org/10.1016/j.chroma.2016.01.064.
613 [56] K. Stejskal, J. Op de Beeck, G. Dürnberger, P. Jacobs, K. Mechtler, Ultrasensitive NanoLC-MS of
614 Subnanogram Protein Samples Using Second Generation Micropillar Array LC Technology with
615 Orbitrap Exploris 480 and FAIMS PRO, Anal. Chem. (2021).
616 https://doi.org/10.1021/acs.analchem.1c00990.
617 [57] D.B. Bekker-Jensen, A. Martínez-Val, S. Steigerwald, P. Rüther, K.L. Fort, T.N. Arrey, A. Harder, A.
618 Makarov, J.V. Olsen, A Compact Quadrupole-Orbitrap Mass Spectrometer with FAIMS Interface
619 Improves Proteome Coverage in Short LC Gradients*, Molecular & Cellular Proteomics. 19 (2020)
620 716–729. https://doi.org/10.1074/mcp.TIR119.001906.
621 [58] M. Gilar, P. Olivova, A.E. Daly, J.C. Gebler, Orthogonality of Separation in Two-Dimensional Liquid
622 Chromatography, Anal. Chem. 77 (2005) 6426–6434. https://doi.org/10.1021/ac050923i.
623 [59] J.M. Davis, D.R. Stoll, P.W. Carr, Effect of First-Dimension Undersampling on Effective Peak
624 Capacity in Comprehensive Two-Dimensional Separations, Analytical Chemistry. 80 (2008) 461–
625 473. https://doi.org/10.1021/ac071504j.
626 [60] T. Kind, K.-H. Liu, D.Y. Lee, B. DeFelice, J.K. Meissen, O. Fiehn, LipidBlast in silico tandem mass
627 spectrometry database for lipid identification, Nature Methods. 10 (2013) 755–758.
628 https://doi.org/10.1038/nmeth.2551.
629 [61] M. Sud, E. Fahy, D. Cotter, K. Azam, I. Vadivelu, C. Burant, A. Edison, O. Fiehn, R. Higashi, K.S. Nair,
630 S. Sumner, S. Subramaniam, Metabolomics Workbench: An international repository for

metabolomics data and metadata, metabolite standards, protocols, tutorials and training, and analysis tools, Nucleic Acids Research. 44 (2016) D463–D470. https://doi.org/10.1093/nar/gkv1042.
[62] M.J. Sorensen, R.T. Kennedy, Capillary ultrahigh-pressure liquid chromatography-mass spectrometry for fast and high resolution metabolomics separations, Journal of Chromatography A. 1635 (2021) 461706. https://doi.org/10.1016/j.chroma.2020.461706.
[63] D.S. Gertner, D.P. Bishop, A. Oglobline, M.P. Padula, Enhancing Coverage of Phosphatidylinositol Species in Canola Through Specialised Liquid Chromatography-Mass Spectrometry Buffer Conditions, Journal of Chromatography A. 1637 (2021) 461860. https://doi.org/10.1016/j.chroma.2020.461860.
[64] Y. Shen, R. Zhang, R.J. Moore, J. Kim, T.O. Metz, K.K. Hixson, R. Zhao, E.A. Livesay, H.R. Udseth, R.D. Smith, Automated 20 kpsi RPLC-MS and MS/MS with Chromatographic Peak Capacities of 1000−1500 and Capabilities in Proteomics and Metabolomics, Analytical Chemistry. 77 (2005) 3090–3100. https://doi.org/10.1021/ac0483062.
[65] M. Baca, G. Desmet, H. Ottevaere, W. De Malsche, Achieving a Peak Capacity of 1800 Using an 8 m Long Pillar Array Column, Anal. Chem. 91 (2019) 10932–10936. https://doi.org/10.1021/acs.analchem.9b02236.
[66] S. Chapel, F. Rouvière, S. Heinisch, Pushing the limits of resolving power and analysis time in on-line comprehensive hydrophilic interaction x reversed phase liquid chromatography for the analysis of complex peptide samples, Journal of Chromatography A. 1615 (2020) 460753. https://doi.org/10.1016/j.chroma.2019.460753.
[67] D.R. Stoll, H.R. Lhotka, D.C. Harmes, B. Madigan, J.J. Hsiao, G.O. Staples, High resolution two-dimensional liquid chromatography coupled with mass spectrometry for robust and sensitive characterization of therapeutic antibodies at the peptide level, Journal of Chromatography B. 1134–1135 (2019) 121832. https://doi.org/10.1016/j.jchromb.2019.121832.